AD-A095 410 BROWN UNIV PROVIDENCE R I ENGINEERING MATERIALS RESE--ETC F/G 11/6
SIMULTANEOUS STRESS RELAXATION IN TENSION AND CREEP IN TORSION --ETC(U)
OCT 80 J S LAI, W N FINDLEY DAAG29-79-G-0185

UNCLASSIFIED EMRL-76 ARO-15508.5-E NL

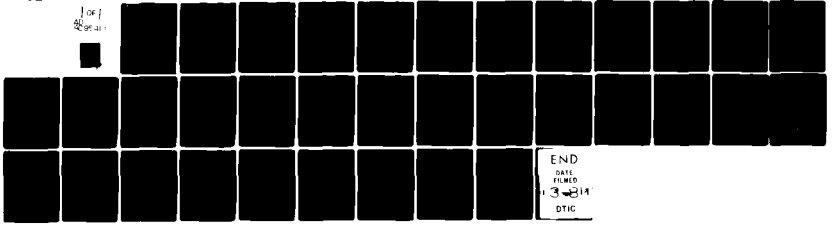

END
DATE FILMED
3-81
DTIC

Division of Engineering
BROWN UNIVERSITY
PROVIDENCE, R. I.

Engineering Materials Research Laboratory

SIMULTANEOUS STRESS RELAXATION IN TENSION AND CREEP IN TORSION OF 2618 ALUMINUM AT ELEVATED TEMPERATURE

James S. Lai and William N. Findley

Army Research Office
Technical Report No. 3
Grant DAAG29-79-G-0185

ARO DAAG29-79-G-0185/3
EMRL-76

October 1980

UNCLASSIFIED
SECURITY CLASSIFICATION OF THIS PAGE (When Data Entered)

AD A095410

REPORT DOCUMENTATION PAGE

READ INSTRUCTIONS BEFORE COMPLETING FORM

1. REPORT NUMBER: (11) 15508.3-E (12) DAAG	2. GOVT ACCESSION NO.: AD-A095 410
3. RECIPIENT'S CATALOG NUMBER:	
4. TITLE (and Subtitle): (6) Simultaneous Stress Relaxation in Tension and Creep in Torsion of 2618 Aluminum at Elevated Temperature.	5. TYPE OF REPORT & PERIOD COVERED: (9) Technical Rept.
	6. PERFORMING ORG. REPORT NUMBER:
7. AUTHOR(s): (10) James S. Lai, William N. Findley (12)	8. CONTRACT OR GRANT NUMBER(s): (15) DAAG29-79-C-0185
9. PERFORMING ORGANIZATION NAME AND ADDRESS: Brown University, Providence, RI 02912 (14)	10. PROGRAM ELEMENT, PROJECT, TASK AREA & WORK UNIT NUMBERS: EMRL-1
11. CONTROLLING OFFICE NAME AND ADDRESS: U. S. Army Research Office, Post Office Box 12211, Research Triangle Park, NC 27709	12. REPORT DATE: Oct 80
	13. NUMBER OF PAGES: 32
14. MONITORING AGENCY NAME & ADDRESS(if different from Controlling Office)	15. SECURITY CLASS. (of this report): Unclassified
	15a. DECLASSIFICATION/DOWNGRADING SCHEDULE

LEVEL II

16. DISTRIBUTION STATEMENT (of this Report)

Approved for public release; distribution unlimited.

17. DISTRIBUTION STATEMENT (of the abstract entered in Block 20, if different from Report)

NA

18. SUPPLEMENTARY NOTES

The view, opinions, and/or findings contained in this report are those of the author(s) and should not be construed as an official Department of the Army position, policy, or decision, unless so designated by other documentation.

19. KEY WORDS (Continue on reverse side if necessary and identify by block number)

creep properties
tensile tests
torsion
aluminum alloys
high temperature
stress relaxation

20. ABSTRACT (Continue on reverse side if necessary and identify by block number)

Experiments are reported for stress relaxation and simultaneous stress relaxation and creep with proportional and non proportional loading and unloading. Results were compared with predictions of a viscous-viscoelastic theory, and modifications, and strain hardening. Predictions were calculated from results of combined constant-stress tension and torsion creep and recovery tests only, which were reported previously. Results showed that a modified viscous-viscoelastic theory predicted all the observed features and predicted the creep and relaxation rates reasonably well.

DD FORM 1 JAN 73 1473 EDITION OF 1 NOV 65 IS OBSOLETE

UNCLASSIFIED
SECURITY CLASSIFICATION OF THIS PAGE (When Data Entered)

FILE COPY

SIMULTANEOUS STRESS RELAXATION IN TENSION AND CREEP IN TORSION OF 2618 ALUMINUM AT ELEVATED TEMPERATURE

by

James S. Lai and William N. Findley

Abstract

Experiments are reported for stress relaxation and simultaneous stress relaxation and creep with proportional and non proportional loading and unloading. Results were compared with predictions of a viscous-viscoelastic theory, and modifications, and strain hardening. Predictions were calculated from results of combined constant-stress tension and torsion creep and recovery tests only, which were reported previously.

Results showed that a modified viscous-viscoelastic theory predicted all the observed features and predicted the creep and relaxation rates reasonably well.

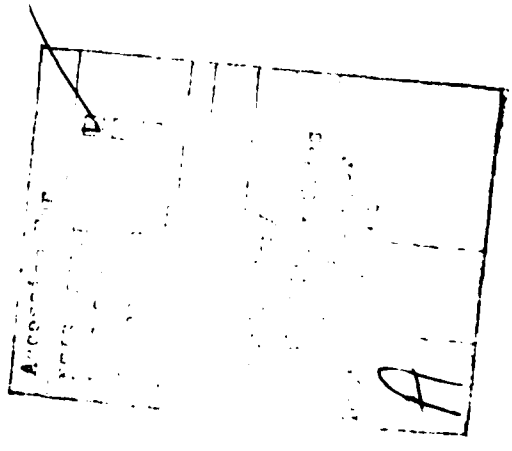

Introduction

The literature on the time-dependent behavior of metals at elevated temperature, mostly deals with creep under uniaxial stress states. Next most numerous are perhaps the works on stress relaxation under simple stress states and least numerous creep under multi-axial stress states. A few have also considered predicting stress relaxation behavior from creep under the same stress state (mostly uniaxial tension). Selected references to the previous investigations of time-dependent behavior of metals under multiaxial stress are given in [1] and [2]. No prior work on simultaneous creep and stress relaxation of metals has been found in the literature. The only investigation of simultaneous creep and relaxation was performed by the authors [3,4] on full density polyurethane.

In previous papers [1,5,6] the authors investigated the creep behavior of 2618 Aluminum at 200°C (392°F) under combined tension and torsion stresses. In the first paper the authors developed constitutive equations to describe the creep behavior of the material under multi-axial stress states. The constitutive equations employed five strain components: linear elastic ε^e; time-independent plastic ε^p; time-dependent positive nonrecoverable ε^v_{pos} and time-dependent negative nonrecoverable ε^v_{neg}; time-dependent recoverable ε^{ve}. From creep and recovery experiments under combined tension and torsion, the time and stress dependence of these components were evaluated [1] for constant stress. In [5,6] the constitutive relations developed for a constant stress state were extended for time-dependent stress histories. The extended constitutive equations were used to predict the creep behavior of the material for combined tension and torsion and under varying stress history, including

step-up and step-down stress changes and repeated reversal of shearing stress with and without constant tension. Paper [5] dealt with simple stress states while paper [6] dealt with combined tension and torsion stress states.

In the present paper, experiments involving simultaneous stress relaxation in tension and creep in torsion are reported and discussed. These experiments were performed on the same lot of 2618 aluminum as the experiments in [1,5,6]. Methods of predicting simultaneous creep in torsion and stress relaxation in tension from the constitutive equations developed in papers [1,5,6] are presented in the present paper. Predictions of stress relaxation and creep under combined tension and torsion stress states using the proposed methods were computed and compared with the experimental results.

Test Material

An aluminum forging alloy 2618-T61 was employed in these experiments. Specimens were taken from the same lot of 63.5 mm (2-1/2 in.) diameter forged rod as used in [1,5,6] and the same lot as specimen D through H in [7]. Specimens were thin-walled tubes having outside diameter, wall thickness and gage length of 25.4, 1.52 and 101.6 mm (1.00, 0.060, and 4.00 inches), respectively. A more complete description of material and specimen is given in [1].

Experimental Apparatus and Procedure

The combined tension and torsion creep machine, Fig. 1, used for the experiments was described in [8] and briefly in [1]. Tension was applied by means of dead weights through lever A, Fig. 1. A system of counter balances

permitted torque in either sense to be applied by adding or removing weight from lever B. The tensile strain was monitored by using an extensometer, C, Fig. 1, attached to the upper and lower gage points of the test specimen. The sensitivity was 1×10^{-6} for tensile strain. Shear strain was measured by a mechanical device, employing a microscope D, Fig. 1, whose sensitivity was 1.5×10^{-6} for tensor shear strain. During a stress relaxation test, the tensile strain was maintained constant by means of a servomechanism whose input was the difference between the voltage generated from the command signal (desired strain level) and that from the actual strain response. The output from the servo-controller drove a servo-valve, E, Fig. 1, which controlled the flow of hydraulic fluid from the pump to the hydraulic cylinder, F, Fig. 1. This cylinder was connected in series with a load cell, G, Fig. 1, and used to apply the load to the test specimen through a hooked rod to a loading lever, A, Fig. 1. The load applied to the specimen was measured by the load cell to a sensitivity of 9 g (0.02 pound).

The specimen, H, Fig. 1, was heated internally by a quartz-tube radiant-heating lamp and externally by two resistance heaters at the ends just outside the gage length. The details of temperature control for the experiment were described in [1,7]. Measurements made during the experiments indicated a temperature variation of ±0.6°C (±1°F) both with time and with position along the gage length of the specimen.

After the set-up, the specimen was soaked at the test temperature of 200°C for approximately 18 hr. prior to testing. The influence of aging on the experimental results, as discussed in [1,5], indicated that during the testing time of the experiments reported the creep rate increased about 1/2 percent per hr., which is considered negligible.

Experimental Results

The results of four combined tension relaxation and torsion creep experiments are shown in Figs. 2 to 5 respectively. The loading and straining programs for each test are shown in inserts on each figure.

In Fig. 2A a constant tensile strain was maintained in period 1 and a typical stress relaxation curve was observed. In periods 2 and 3, Fig. 2, a constant torque was added and removed while the tensile strain was kept constant. In period 2, Fig. 2A, a new primary-type relaxation occurred. The rate of the stress relaxation continued unchanged into period 3 upon removal of the torque. In Fig. 2B, the usual shape of creep and recovery behavior were observed for the shear strain for period 2 and 3. In the fourth period, Fig. 2, the tensile stress (not the strain) became zero. The reason that the specimen did not recover at zero strain was that the testing machine was not designed to take a compressive force. If the specimen were to recover at zero tensile strain a compressive force would have been required.

The experiment in Fig. 3 involved simultaneously applying constant strain in tension and constant shearing stress in torsion in the first period. Stress relaxation in tension and creep in torsion were observed as shown in Fig. 3A and 3B respectively. In the second period, Fig. 3, the shearing stress was increased about 10 percent while the tensile strain remained constant. The results shown indicate that both the stress relaxation and creep behaviors in period 2 continued without significant change in character from the first period. In period 3, the tensile strain was kept constant while the shearing stress was removed. The rate of

stress relaxation in period 3 Fig. 3A continued essentially unchanged from that in period 2. The usual recovery of the shear strain in period 3 Fig. 3B was observed. In the subsequent periods, a constant shearing stress was repeatedly added and removed three times while the tensile strain was kept constant. In Fig. 3A, periods 4, 6, and 8, (when the shearing stress was on), the stress relaxation behaved as if the shear stress were on continuously from period 4 to 8 (not influenced by the intervals of unloading). Period 5 showed a continued relaxation while period 7 showed a rebound in stress. Other instances of rebound occurred in periods 3 and 5, Fig. 4A. In Fig. 3B, the successive loadings in periods 4, 6, and 8 resulted in decreasing creep rates. In periods 5 and 7, recovery was observed.

In Fig. 4 the first three periods are similar to those of Fig. 2A except for a higher tensile strain (0.29%). The responses of the first three periods in this test were very similar to those shown in Fig. 2. In periods 4 and 5, a constant shearing stress (greater than the shearing stress in period 2) was added and removed. A rapid stress relaxation was observed in period 4, Fig. 4A, while a small increase in stress was observed in periods 3 and 5. The results in period 4 of Fig. 4A and periods 4, 6, and 8 of Fig. 3A indicate that upon reloading in torsion to a higher value while keeping the tensile strain constant, a rapid tensile stress relaxation resulted. On the other hand, if the reloading of torsion was to the same magnitude, the rate of tensile stress relaxation continued as if the shear stress was uninterrupted. In Fig. 4B, periods 4 and 5 characteristic creep and recovery behavior were observed.

Fig. 5 involved simultaneously applying constant tensile strain and shearing stress in period 1. In period 2 the tensile stress was removed while the shearing stress was kept constant. This was followed by removal of shearing stress in period 3. Characteristic stress relaxation in tension and creep in torsion were observed in period 1. In period 2, Fig. 5B upon removal of tensile "stress," the creep in torsion was continued as if no removal of tensile "stress" had occurred. In period 3, Fig. 5B, a recovery in shear strain was observed. In periods 2 and 3 Fig. 5A the stress was reduced to zero rather than the strain being reduced to zero. Thus no further stress relaxation occurred. Instead a "creep" recovery occurred at zero stress which is not shown.

In the following sections the constitutive equations developed in [1,5,6] for creep behavior of the same material are presented and used to predict the stress relaxation and creep behaviors shown above.

Discussion of Experimental Results; Comparison with Combined Stress Creep

A comparison of the results of the present experiments on histories of variable simultaneous relaxation in tension and creep in torsion shows similar features to those found in variable combined tension and torsion creep [6]. Among these similar features are the following: (a) When a shearing stress τ was added to a tensile relaxation at a constant tensile strain ε_{11} a new "primary" type stress relaxation resulted as in period 2 Fig. 2A, and periods 2 and 4 Fig. 4A. (b) When the shearing stress τ was removed to zero while the tensile strain ε_{11} remained constant there was no significant change in the pattern of stress relaxation in tension as shown in period 3 Fig. 2A. Similar but not as well defined behavior is

also shown in period 3 Fig. 3A, and periods 3 and 5 Fig. 4A. (c) When the tensile stress σ was changed to zero during tensile relaxation while the shearing stress remained constant the creep ε_{12} continued as though there had been no change. See period 2 Fig. 5B. (d) When the tensile stress was changed to zero following constant strain relaxation while the shearing strain ε_{12} was recovering from prior creep at a shearing stress τ a new recovery type behavior was initiated in ε_{12} as shown in period 4 Fig. 2B.

Constitutive Equations for Creep Under Combined Tension and Torsion

In the previous papers [1,5,6] it was shown that creep of specimens of the same lot of 2618 Aluminum at 200°C under combined tension and torsion were adequately described by the following relation:

$$\varepsilon_{ij}(t) = \varepsilon_{ij}^{e} + \varepsilon_{ij}^{p} + \varepsilon_{ij}^{v}(t) + \varepsilon_{ij}^{ve}(t) \quad , \tag{1}$$

where ε_{ij}^{e}, ε_{ij}^{v}, and ε_{ij}^{ve} represent the time-independent elastic strain, time-dependent nonrecoverable (viscous) strain and time-dependent recoverable (viscoelastic) strain, respectively, and ε_{ij}^{v} was further resolved into positive and negative components. The time-independent plastic strain ε_{ij}^{p} was found to be zero in the experiments. The elastic modulus E_o, shear modulus G_o and Poisson's Ratio ν for the elastic strain component ε^{e} for the material at 200°C as reported in [1,5,6] is given in Table 1. The constitutive relations for $\varepsilon_{ij}^{v}(t)$ and $\varepsilon_{ij}^{ve}(t)$ under constant stresses and time-dependent stresses as employed in [1,5,6] are reviewed in the following.

Constant Stress

Under constant stress, the components ε^{v} and ε^{ve} under combined tension σ and torsion τ were represented by the following equations:

$$\varepsilon_{11}^{ve}(t) = \left(\frac{R}{1+R}\right) F\,[(\sigma-\sigma'),(\tau-\tau')]t^{n} \quad , \tag{2}$$

$$\varepsilon_{12}^{ve}(t) = \left(\frac{R}{1+R}\right) G\,[(\sigma-\sigma'),(\tau-\tau')]t^{n} \quad , \tag{3}$$

$$\varepsilon_{11}^{v}(t) = \left(\frac{1}{1+R}\right) F\,[(\sigma-\sigma'),(\tau-\tau')]t^{n} \quad , \tag{4}$$

$$\varepsilon_{12}^{v}(t) = \left(\frac{1}{1+R}\right) G\,[(\sigma-\sigma'),(\tau-\tau')]t^{n} \quad . \tag{5}$$

The nonlinear functions of F and G in (2-5) were derived from a third order multiple integral representation [4], where

$$\begin{aligned} F(\sigma-\sigma',\tau-\tau') = {} & F_1(\sigma-\sigma') + F_2(\sigma-\sigma')^2 + F_3(\sigma-\sigma')^3 \\ & + F_4(\sigma-\sigma')(\tau-\tau')^2 + F_5(\tau-\tau')^2 \quad , \end{aligned} \tag{6}$$

$$\begin{aligned} G(\sigma-\sigma',\tau-\tau') = {} & G_1(\tau-\tau') + G_2(\tau-\tau')^3 + G_3(\sigma-\sigma')(\tau-\tau') \\ & + G_4(\sigma-\sigma')^2(\tau-\tau') \quad , \end{aligned} \tag{7}$$

and σ', τ' are the components of the creep limit. In the original formulation [1], a Tresca form, as shown in the following, was employed for the creep limits (σ' and τ') under combined tension-torsion stresses,

$$\begin{aligned} (\sigma')^2 + 4(\tau')^2 = (\sigma^*)^2 = (2\tau^*)^2 \quad , \\ \sigma'/\sigma = \tau'/\tau \quad , \end{aligned} \tag{8}$$

where σ^* and τ^* are the creep limits under pure tension and pure torsion respectively. The coefficients of F_i, G_i, and values of σ^*, τ^*, R and n were derived from constant combined tension-torsion creep and recovery tests reported in [1] and shown in Table I. The values of the coefficients corresponding to (6-8) were given in [1] and corrected in [5].

It was shown in [6] that using the variable creep limits σ', τ' and (8) did not predict the experimental results quite as accurately as using fixed creep limits σ^* and τ^*. In the present paper, calculations were made using the fixed creep limits, σ^* and τ^*, as well as σ', τ'. The calculations of the predicted creep and relaxation curves shown in Fig. 2-5 are for σ', τ'. Similar calculations made for the fixed creep limits σ^*, τ^* are not shown. The results were somewhat better for σ', τ' than σ^*, τ^* and are more generally applicable.

Time-Dependent Stress

The modified superposition principle (MSP) as derived from the multiple integral representation was shown in [3.4] to be able to describe time-dependent recoverable (viscoelastic) strain. Under a continuously varying stress σ, the strain response ε^{ve} given by the modified superposition principle was represented for nonlinear behavior in [5,6] by

$$\varepsilon_{ij}^{ve}(t) = \int_0^t \frac{\partial}{\partial\sigma(\xi)} f_{ij}[\bar{\sigma}(\xi),\bar{\tau}(\xi),t-\xi]\dot{\bar{\sigma}}(\xi)\, d\xi \quad , \tag{9}$$

where $f_{ij}(\sigma,t)$ represents the nonlinear-stress and time-dependent creep function such as (2) and (3) for ε_{11}^{ve} and ε_{12}^{ve} respectively, and where $\bar{\sigma}(t) = \sigma(t) - \sigma'$ and $\bar{\tau}(t) = \tau(t) - \tau'$. For a series of m step changes in stress as employed in the present work, (9) becomes as follows for ε_{12}^{ve} for example:

$$\begin{aligned}\varepsilon_{12}^{ve}(t) = (\tfrac{R}{1+R})\{&G(\bar{\sigma}_1,\bar{\tau}_1)[t^n-(t-t_1)^n] + \ldots \\ &+ G(\bar{\sigma}_{m-1},\bar{\tau}_{m-1})[(t-t_{n-2})^n-(t-t_{m-1})^n] \\ &+ G(\bar{\sigma}_m,\bar{\tau}_m)(t-t_{m-1})^n\} \quad , \quad t_{m-1} < t \quad .\end{aligned} \tag{9a}$$

For the time-dependent nonrecoverable (viscous) strain component ε^v, it was shown in [5,6] that a strain hardening theory reasonably described the behavior of this strain component under a time-dependent stress input. The strain-hardening theory for ε_{11}^{ve} and ε_{12}^{ve} can be represented by the following equations:

$$\varepsilon_{11}^{v}(t) = \frac{1}{1+R}\left[\int_0^t \{F[\bar{\sigma}(\xi),\bar{\tau}(\xi)]\}^{1/n}\, d\xi\right]^n \quad , \tag{10}$$

$$\varepsilon_{12}^{v}(t) = \frac{1}{1+R}\left[\int_0^t \{G[\bar{\sigma}(\xi),\bar{\tau}(\xi)]\}^{1/n}\, d\xi\right]^n \quad . \tag{11}$$

Equations (10) and (11) were derived from (4) and (5), respectively, using the strain-hardening concept as described in [1,5].

For a series of m step changes in stress, as employed in the present paper, (11) for example becomes as follows:

$$\varepsilon_{12}^{v}(t) = \left(\frac{1}{1+R}\right)\{[G(\bar{\sigma}_1,\bar{\tau}_1)]^{1/n}(t_1) + \ldots + [G(\bar{\sigma}_{m-1},\bar{\tau}_{m-1})]^{1/n}(t_{m-1}-t_{m-2}) + [G(\bar{\sigma}_n,\bar{\tau}_m)]^{1/n}(t_{m-1})\}^n \quad , \quad t_2 < t \quad . \tag{12}$$

Viscous-Viscoelastic (VV) Theory

The total strain following a time-dependent stress history was found according to (1) by adding to the elastic strain corresponding to the stresses existing at the time of interest the ε^{ve} given by (9) and the ε^v given by (10) or (11) for axial strain or shear strain. Thus,

$$\varepsilon_{11}(t) = \frac{\sigma}{E} + \frac{1}{1+R}\left[\int_0^t \{F[\bar{\sigma}(\xi),\bar{\tau}(\xi)]\}^{1/n}\, d\xi\right]^n + \frac{R}{1+R}\int_0^t \frac{\partial}{\partial\sigma(\xi)} F[\bar{\sigma}(\xi),\bar{\tau}(\xi),\ t-\xi]\dot{\sigma}(\xi)d\xi \quad , \tag{13a}$$

$$\varepsilon_{12}(t) = \frac{\tau}{2G} + \frac{1}{1+R}\left[\int_0^t \{G[\bar{\sigma}(\xi),\bar{\tau}(\xi)]\}^{1/n}\, d\xi\right]^n + \frac{R}{1+R}\int_0^t \frac{\partial}{\partial\sigma(\xi)} G[\bar{\sigma}(\xi),\bar{\tau}(\xi),t-\xi]\dot{\bar{\tau}}(\xi)\, d\xi \quad , \tag{13b}$$

where E and G are the elastic modulus and shear modulus respectively.

Modified Viscous-Viscoelastic (MVV) Theory

In [5,6] it was found under partial unloading that the observed characteristics of creep behavior of the material were not properly predicted by the VV theory. It was found, however, that the MVV theory employed in [5] described the creep behavior of the material under partial unloading more closely than the VV theory. In the following, the MVV theory, which will be used also in this paper, is reviewed. The basic difference between the MVV and the VV theories is in the treatment of the creep limits for the recoverable strain ε^{ve}. These differences in treatment are illustrated in Fig. 6.

(A) For the nonrecoverable strain component, the strain hardening rule was employed. Upon reduction of stress from σ_A to a current stress σ_B, Fig. 6(a), the strain rate $\dot{\varepsilon}^v$ continued at the reduced (positive) rate prescribed by the strain hardening rule, (10) and (11), as shown in Fig. 6(a), unless the current stress σ_C equaled or was less than the creep limit σ^* (or σ'). When $\sigma_C \leq \sigma^*$ (or σ'), $\dot{\varepsilon}^v$ was zero as prescribed by (10) and (11), see Fig. 6(a).

(B) Upon reloading from a stress σ_C below to a stress σ_D above the creep limit, the nonrecoverable strain rate $\dot{\varepsilon}^v$ resumed at the rate prescribed by (10) and (11) but as though there had been no interval t_x for which $\sigma_C \leq \sigma^*$ (or σ'), see Fig. 6(c).

(C) For the recoverable strain component ε^{ve} on partial unloading the recoverable strain rate $\dot{\varepsilon}^{ve}$ became and remained zero for all reductions of stress from σ_A to σ_B, as shown in Fig. 6(b) unless the total change in stress from the highest stress σ_{max} [$=\sigma_A$ in Fig. 6(b)] previously encountered to the current stress σ_C equaled in magnitude the creep limit σ^* (or σ'). That is,

$$\dot{\varepsilon}^{ve} = 0 \quad \text{when} \quad (\sigma_A - \sigma_B) \leq |\sigma^*| \text{ (or } \sigma') \quad , \tag{14}$$

$$\dot{\varepsilon}^{ve} \neq 0 \quad \text{when} \quad (\sigma_A - \sigma_C) > |\sigma^*| \text{ (or } \sigma') \quad . \tag{15}$$

Equation (14) can be considered as meaning that for a small unloading the recoverable strain component was "frozen." Equation (15) indicates that if the change in stress was greater than $|\sigma^*|$ or $|\sigma'|$ then recovery would occur followed eventually by creep, see Fig. 6(b).

(D) Upon increasing the stress to σ_D ($\sigma_D \geq \sigma_A$) following a period t_x (a dead zone) for which $(\sigma_{max} - \sigma_B) \leq |\sigma^*|$ (or σ') and $\dot{\varepsilon}^{ve} = 0$, as discussed in (C) above, the recoverable strain component ε^{ve} continued to creep in accordance with the viscoelastic behavior (9) as though the period t_x never occurred, see Fig. 6(c). In computing the behavior for situations described in (B), (C) and (D) it was thus necessary to introduce a time shift in equations (9), (10) or (11) to eliminate the appropriate period t_x when ε^{ve} was "frozen." Thus, the new time t' subsequent to a period $t_x = (t_b - t_a)$ becomes $t' = t - (t_b - t_a)$, where t is the real time and t_a, t_b are the times when σ_A was removed and σ_D was applied.

(E) When recoverable and nonrecoverable strain components are considered together two special circumstances arise. Consider that the stress decreases from the highest value σ_A to a lower value σ_B under a uniaxial stress state. If $\sigma_A > 2\sigma^*$ and $\sigma^* \leq \sigma_B \leq (\sigma_A - \sigma^*)$ then there is creep occurring from ε^v and

recovery from ϵ^{ve}. However, if $\sigma_A < 2\sigma^*$ and $(\sigma_A - \sigma^*) < \sigma_B < \sigma^*$ then there is neither creep nor recovery, $\dot{\epsilon}^{v} = \dot{\epsilon}^{ve} = 0$.

(F) When one stress component decreased while the other remained constant the recoverable strain component ϵ^{ve} was treated as follows. The material behavior in such situations suggested that reducing or removing one stress component, say τ, while the other component, say σ, remained constant affected the strain as follows. The strain corresponding to mixed stress components behaved as though these mixed components had suffered a small stress reduction. That is, the strain, say ϵ_{11}, associated with the mixed stress components, say $\sigma\tau^2$, τ^2, became constant. The strain, say ϵ_{11}, associated with the pure stress terms, say σ, σ^2, σ^3 which were unchanged, continued as though nothing had happened.

Strain-Hardening (SH) Theory

The total strain under this theory can be represented by the following equations according to (10) and (11)

$$\epsilon_{11}(t) = \frac{\sigma(t)}{E} + \left[\int_0^t \{F[\bar{\sigma}(\xi), \bar{\tau}(\xi)\}^{1/n} \, d\xi\right]^n , \tag{16}$$

$$\epsilon_{12}(t) = \frac{\tau(t)}{2G} + \left[\int_0^t \{G[\bar{\sigma}(\xi), \tau(\bar{\xi})\}^{1/n} \, d\xi\right]^n . \tag{17}$$

Prediction of Simultaneous Creep in Torsion and Relaxation in Tension From Combined Stress Creep Data

Since creep and stress relaxation behaviors are two aspects of time-dependent behavior of materials, one behavior should be predictable if the other behavior is known. In other words, in a "tensile stress relaxation" test for example, the stress response of a material under a constant axial strain input may be considered as equivalent to a tensile "creep" test

with an undetermined time-dependent stress applied to the specimen such that a constant axial strain results throughout the testing period. The prediction of simultaneous creep and relaxation from combined stress creep to be described in the following is based on this premise.

Some investigators have considered a relaxation test to be fundamentally different from a creep test - that the material has a constant strain state in relaxation compared to a changing strain state in creep. However, the strain state is not constant during a relaxation test. In an axial relaxation test only the axial strain component remains constant while the transverse strains are time dependent [4] unless the relaxation is volume constant, which is not true in general. On the other hand, in a constant-stress creep test all stress components are constant.

The simultaneous stress relaxation in tension and creep in torsion when the specimen is subjected to constant tensile strain and constant shearing stress in torsion can be considered as one of combined tension and torsion creep with variable (time-dependent) tensile stress and constant shearing stress in torsion. The desired time-dependent tensile stress $\sigma(t)$ is unknown. This unknown stress $\sigma(t)$ has to satisfy the condition that the tensile strain produced by the prescribed constant shearing stress and this unknown varying tensile stress $\sigma(t)$ acting together on the specimen must equal the prescribed constant tensile strain. For the VV theory this is equivalent to solving the nonlinear equation (13a) for $\sigma(t)$ with ε_{11} and $\tau(t)$ prescribed. Once $\sigma(t)$ has been determined from (13a), the corresponding shearing strain can be obtained from (13b).

The iterative procedures used to solve for $\sigma(t)$ from (13a) for the VV theory with prescribed tensile strain $\varepsilon_{11}(t)$ and shearing stress $\tau(t)$ are

described in the following. According to this numerical procedure, the prescribed $\epsilon_{11}(t)$ and $\tau(t)$ were divided into a number k of intervals of time (m=1,...k). In the first step the $\epsilon_{11}(1)$ and $\tau(1)$ were known. Neglecting the time-dependent responses, the initial tensile stress $S(1) = \epsilon_{11}(1)\, E$ was determined. With S(1) and $\tau(1)$ for the first step, the $S(t_1)$ and $\tau(t_1)$ at the end of the first interval were computed from (13a). Similarly with $S(t_{m-1})$ at the end of the m-1 interval the $S(t_m)$ and $\tau(t_m)$ were determined from (13a) using the entire stress history from $t = 0$ to $t = t_m$. The difference between the computed tensile strain and the prescribed tensile strain for the m^{th} interval, $\Delta e(t_m) = e(t_m) - \epsilon_{11}(t_m)$ was computed. $\epsilon_{11}(t_m)$ represented the prescribed tensile strain at $t = t_m$. The $\Delta e(t_m)$ was used to determine the correction for the assumed tensile stress $S(t_m)$. Thus, the corrected tensile stress $\sigma(t_m)$ equals $[S(t_m) - \Delta e(t_m)]\, E$. The correction was based on the elastic response only. $\sigma(t_m)$ so determined represented the relaxation stress at $t = t_m$. This corrected tensile stress history $\sigma(t)$ and the prescribed shearing stress history $\tau(t)$ for $t = 0 \rightarrow t_m$ were used to compute the shearing strain using (13b) for the VV theory.

In the next step ($t = t_{m+1}$), the approximate tensile stress $S(t_{m+1})$ was determined by $S(t_{m+1}) = \sigma(t_m) + [\epsilon_{11}(t_{m+1}) - \epsilon_{11}(t_m)]\, E$. For a constant strain relaxation condition, $\epsilon_{11}(t_{m+1}) = \epsilon_{11}(t_m)$, thus, $S(t_{m+1}) = \sigma(t_m)$. The $S(t_{m+1})$ along with the previous tensile stress history $\sigma(t)$, and the shearing stress history $\tau(t)$ for t from 0 to t_{m+1} were used again to compute the tensile strain response $e(t_{m+1})$ using (13a). From that the relaxational stress at $t = t_{m+1}$ was determined.

When using the MVV theory the procedure was almost identical to that described above except the modifications (C), (D), and (F) described in the preceeding section were properly incorporated. For example, when

predicting the relaxational stress in periods 1, 2 and 3 of the test program shown in Fig. 2A, the third term (ε_{11}^{ve}) on the right side of (13a) became zero, because a stress relaxation can be considered as a small partial unloading in a creep test, thus according to (C) of the MVV theory, $\dot{\varepsilon}^{ve} = 0$. For predicting $\varepsilon_{12}(t)$ of periods 2 and 3 of the test program shown in Fig. 2A, the $G(\bar{\sigma},\bar{\tau})$ function in the third term of the right side of (13b) contained two terms $G_1\bar{\tau}$ and $G_2\bar{\tau}^3$ instead of four terms as shown in (7), according to (F) of the MVV theory.

When using the SH theory for the predictions, equations (13a) and (13b) used in the VV theory were replaced by (16) and (17), respectively.

The procedures described above were employed to calculate the response of the simultaneous stress relaxation in tension and creep in torsion of 2618 aluminum at 200°C for the histories shown in Fig. 2-5. In using these procedures it was found that the time interval selected could affect the numerical accuracy. A sensitivity analysis was conducted to determine the affect of time interval on the accuracy of the numerical computations. It was found that close to the region where the $\varepsilon_{11}(t)$ changed abruptly a time interval greater than 0.001 hr. could significantly affect the accuracy of the predictions. Consequently in all the predictions carried out in this program, the time interval was chosen to be 0.001 hr.

Comparison of Predictions with Experimental Results

Creep: As shown in Fig. 2B, 3B, 4B, and 5B, the prediction of the shearing creep component (strain ε_{12}) for the first application for shear stress τ compared well with the test data. This was true for all three theories. As noted before these predictions were based on the numerical constants determined entirely from creep and recovery tests under constant combined

tension and torsion and given in Table 1. All of these experiments in Fig. 2-5 included relaxation in tension simultaneously with the shearing creep. In Fig. 3B and 5B the creep and relaxation started simultaneously, while in Fig. 2B and 4B the relaxation started before the shearing stress was added.

For subsequent periods the shearing strain was reasonably well predicted by either the VV or MVV theories, but not properly predicted by the SH theory when the shearing stress was removed. The MVV theory was lower than the VV theory when tensile relaxation preceeded the torsion creep. No prediction was made for periods 4 Fig. 2B or periods 2 and 3 Fig. 5B because the recovery of ε_{11} was at constant stress rather than constant strain. The creep in period 4 Fig. 4B was not well predicted. This is consistent with the observation for combined stress creep under multiple stress changes at high stresses [6], that the predicted creep rate was too low.

Relaxation: Figures 2A, 3A, 4A and 5A show that the prediction of the magnitude of the tensile relaxation for the first two periods compared with the test data about as well as the comparison for the creep component of the same tests. The best comparison of magnitudes was found with the VV theory (the SH theory was usually nearly the same).

In Fig. 3A and 5A the stress relaxation and creep started simultaneously. In Fig. 2A and 4A the creep (shear stress τ) started one hour after the start of relaxation. In this case the predicted relaxation rate was somewhat greater than observed and not as close to the test data as in Fig. 3A and 5A.

When the torque was removed while the tensile strain remained constant, the VV theory predicted a reversal of the relaxation which was not observed,

see period 3 Fig. 2A, periods 3, 5 and 7 Fig. 3A and periods 3 and 5 Fig. 4A. This was due to the same feature of the theory that caused a prediction of recovery that was not observed in combined tension-torsion creep when one component went to zero. The reversal of relaxation predicted by the VV theory was due to the fact that, upon removal of torque, the last two terms in (6) vanish. This caused a sudden drop in the tensile strain rate. In order to maintain the constant strain imposed by the test program, the tensile stress had to increase accordingly. The SH theory predicted no change in stress and the MVV theory predicted a small decreasing stress but not as much as observed in period 3 Fig. 2A for example.

General: The MVV theory predicted the character of all of the various features of the test results for both the creep and relaxation components. On the other hand the VV theory predicted a trend opposite to that observed during relaxation when the shearing stress was removed while the tensile strain remained constant. The SH theory failed to predict the observed recovery when the shearing stress went to zero.

Comparing the magnitudes of creep strains or relaxation stresses predicted with the observed values shows that the MVV theory usually predicted higher stresses in relaxation and higher strains in creep than the observed values and generally higher values than predicted by the VV and SH theories.

However, if comparison is made on the basis of time dependence alone, that is on the basis of creep or relaxation rate, it may be shown that in general the prediction of the MVV theory is the best. The MVV theory was best or the same in this respect as the VV theory in the following: Fig. 2; Fig. 3 (except Fig. 3A period 4); Fig. 4 (except Fig. 4A period 4, Fig. 4B period 4) and Fig. 5.

All curves shown in Fig. 2-5 employed variable creep limits σ', τ' (8). The use of fixed values of σ^* and τ^* for creep limits yielded differences which were sometimes improvements and sometimes not. Since fixed values of σ^*, τ^* lose their meaning for stress states in which one component is below the creep limit the results for fixed creep limits are not shown in the Figures.

Conclusions

Results of experiments on simultaneous creep in torsion and relaxation in tensions were presented. These included proportional and non-proportional loading, unloading and reloading. In general the features of the material response were similar to those observed under combined tension and torsion creep.

Three theories were used to predict the material response to the several mixed load-constraint histories tested. These predictions were made using the results of constant load creep and recovery experiments under combined tension and torsion only. Results showed that a modified viscous-viscoelastic (MVV) theory predicted all the observed features and in general had the best prediction of creep and relaxation rates.

Acknowledgment

This work was supported by the Army Research Office Research Grant No. DAAG29-79-G-0185. The material was contributed by the Aluminum Company of America. The authors are grateful to C. Kang for performing the experiments and P. Orzechowski for typing the manuscript.

References

1. Findley, W. N., and Lai, J. S., "Creep and Recovery of 2618 Aluminum Alloy Under Combined Stress with a Representation by a Viscous-Viscoelastic Model," Trans. ASME, Journal of Applied Mechanics, Vol. 45, Sept. 1978, pp. 507-514.

2. Findley, W. N., Cho, U. W., Ding, J. L., "Creep of Metals and Plastics under Combined Stresses, A Review," ASME Journal of Engineering Materials and Technology, Vol. 101, 1979, p. 365.

3. Lai, J. S., and Findley, W. N., "Behavior of Nonlinear Viscoelastic Material Under Simultaneous Stress Relaxation in Tension and Creep in Torsion," Trans. ASME, J. Appl. Mech., Vol. 36E, 1969.

4. Findley, W. N., Lai, J. S., and Onaran, K., Creep and Relaxation of Nonlinear Viscoelastic Materials, North-Holland Publishers, 1976.

5. Lai, J. S., and Findley, W. N., "Creep of 2618 Aluminum Under Step Stress Changes Predicted by a Viscous-Viscoelastic Model," Trans. ASME, Journal of Applied Mechanics, Vol. 47, March 1980, pp. 21-26.

6. Findley, W. N., and Lai, J. S., "Creep of 2618 Aluminum Under Side Steps of Tension and Torsion and Stress Reversal Predicted by a Viscous-Viscoelastic Model," Trans. ASME, Journal of Applied Mechanics, in press.

7. Blass, J. J., and Findley, W. N., "Short-Time Biaxial Creep of an Aluminum Alloy with Abrupt Changes of Temperature and State of Stresses," Journal of Applied Mechanics, Trans. ASME, Vol. 38, Series E, No. 2, June 1971, pp. 489-501.

8. Findley, W. N., and Gjelsvik, A., "A Biaxial Testing Machine for Plasticity, Creep or Relaxation Under Variable Principle-Stress Ratios," Proc. American Society for Testing and Materials, Vol. 62, 1962, pp. 1103-1118.

Table I. Constants for Equations (2) through (13) Using σ' , τ' for F_4^+ , G_3^+ and G_4^+

F_1^+ =	6.084×10^{-12}, per Pa-h^n (0.004195, % per ksi-h^n)
F_2^+ =	-7.431×10^{-20}, per Pa^2-h^n (-0.0003533, % per ksi^2-h^n)
F_3^+ =	7.596×10^{-28}, per Pa^3-h^n (0.0000249, % per ksi^3-h^n)
σ^* =	9.143×10^7, Pa (13.26, ksi)
G_1^+ =	7.170×10^{-12}, per Pa-h^n (0.004944, % per ksi-h^n)
G_2^+ =	2.703×10^{-28}, per Pa^3-h^n (0.00000886, % per ksi^3-h^n)
τ^* =	4.571×10^7, Pa (6.630, ksi)
F_4^+ =	1.0491×10^{-28}, per Pa^3-h^n (0.000003439, % per ksi^3-h^n)
F_5^+ =	0
G_3^+ =	-4.020×10^{-20}, per Pa^2-h^n (-0.0001911, % per ksi^2-h^n)
G_4^+ =	9.222×10^{-28}, per Pa^3-h^n (0.00003023, % per ksi^3-h^n)

Note: $n = 0.270$
$R = 0.55$
$E = 6.5 \times 10^4$ MPa (9.43×10^6 psi)
$G = 2.45 \times 10^4$ MPa (3.57×10^6 psi)
$\nu = 0.321$

Figure Captions

Fig. 1 Apparatus for Simultaneous Stress Relaxation in Tension and Creep in Torsion.

Fig. 2A Stress Relaxation in Tension with and without Added Torsion.
τ_1 = 79.63 MPa (11.55 ksi)

Fig. 2B Creep in Torsion During Stress Relaxation in Tension.
τ_1 = 79.63 MPa (11.55 ksi)

Fig. 3A Stress Relaxation in Tension Simultaneously with a Program of Creep in Torsion.
τ_1 = 55.50 MPa (8.05 ksi)
τ_2 = 61.01 MPa (8.85 ksi)
τ_3 = 79.63 MPa (11.55 ksi)

Fig. 3B Creep in Torsion During Stress Relaxation in Tension.
τ_1 = 55.50 MPa (8.05 ksi)
τ_2 = 61.01 MPa (8.55 ksi)
τ_3 = 79.63 MPa (11.55 ksi)

Fig. 4A Stress Relaxation in Tension with Periods of Added Torsion.
τ_1 = 79.63 MPa (11.55 ksi)
τ_2 = 95.55 MPa (13.86 ksi)

Fig. 4B Creep in Torsion During Stress Relaxation in Tension.
τ_1 = 79.63 MPa (11.55 ksi)
τ_2 = 95.55 MPa (13.86 ksi)

Fig. 5A Stress Relaxation in Tension Simultaneously with Creep in Torsion.
τ_1 = 79.63 MPa (11.55 ksi)

Fig. 5B Creep in Torsion Simultaneously with Stress Relaxation in Tension.
τ_1 = 79.63 MPa (11.55 ksi)

Fig. 6 Illustration of the Role of the Creep Limit in Partial Unloading and Reloading.

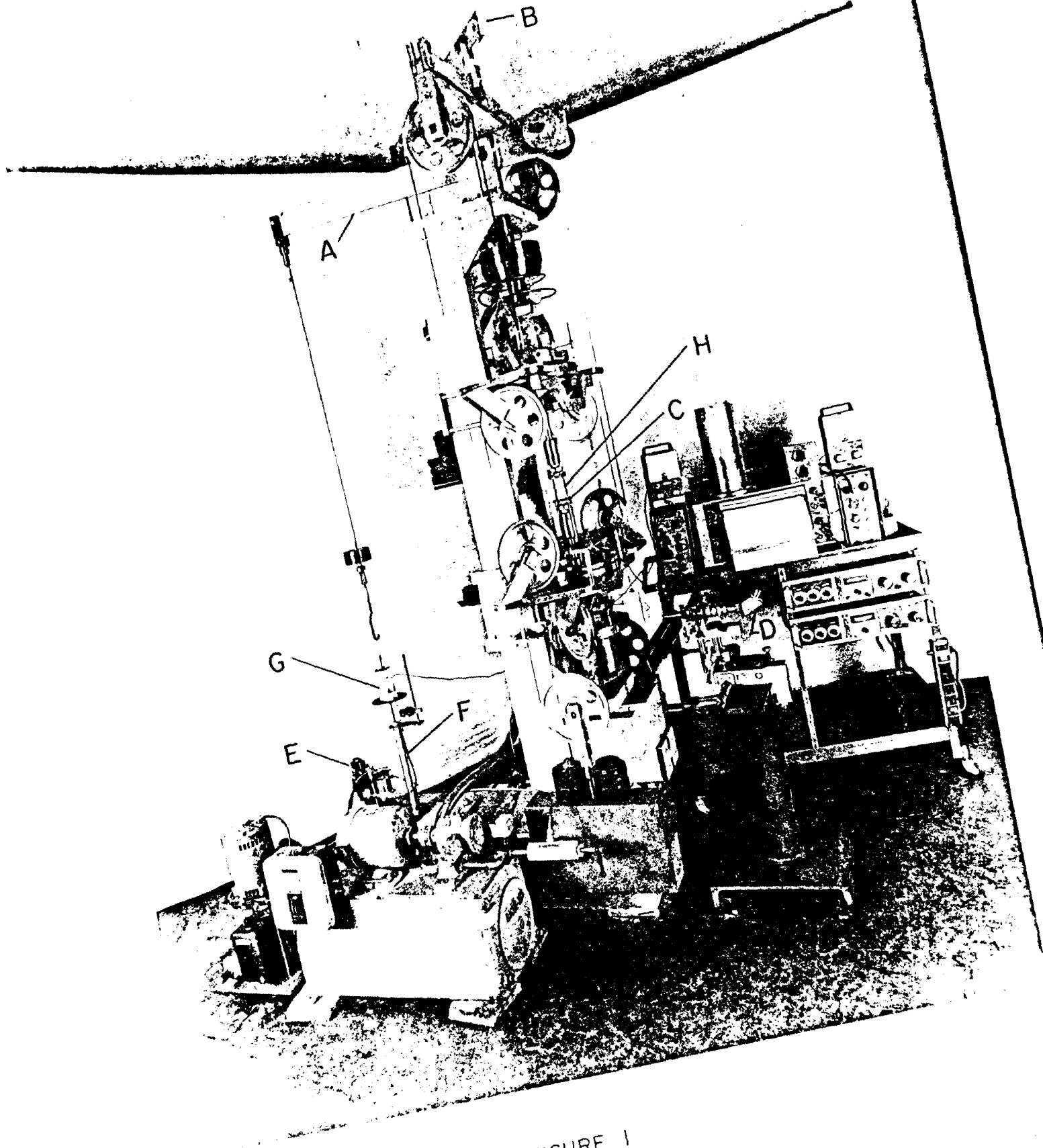

FIGURE 1

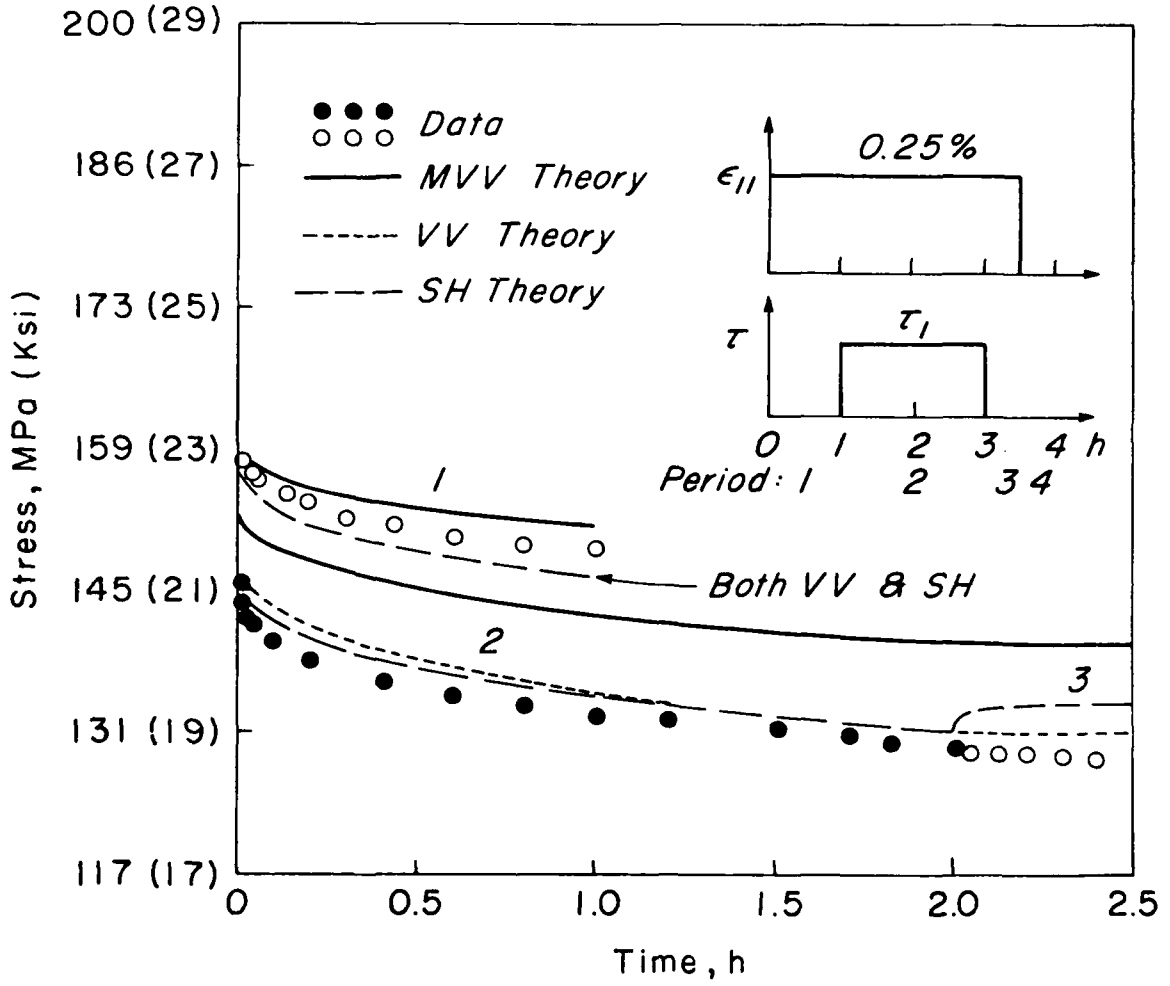
200 (29)
186 (27)
173 (25)
159 (23)
145 (21)
131 (19)
117 (17)
Stress, MPa (Ksi)
0
0.5
1.0
1.5
2.0
2.5
Time, h
Data
MVV Theory
VV Theory
SH Theory
0.25%
ϵ_{11}
τ
τ_1
0 1 2 3 4 h
Period: 1 2 3 4
1
2
3
Both VV & SH

FIGURE 2A

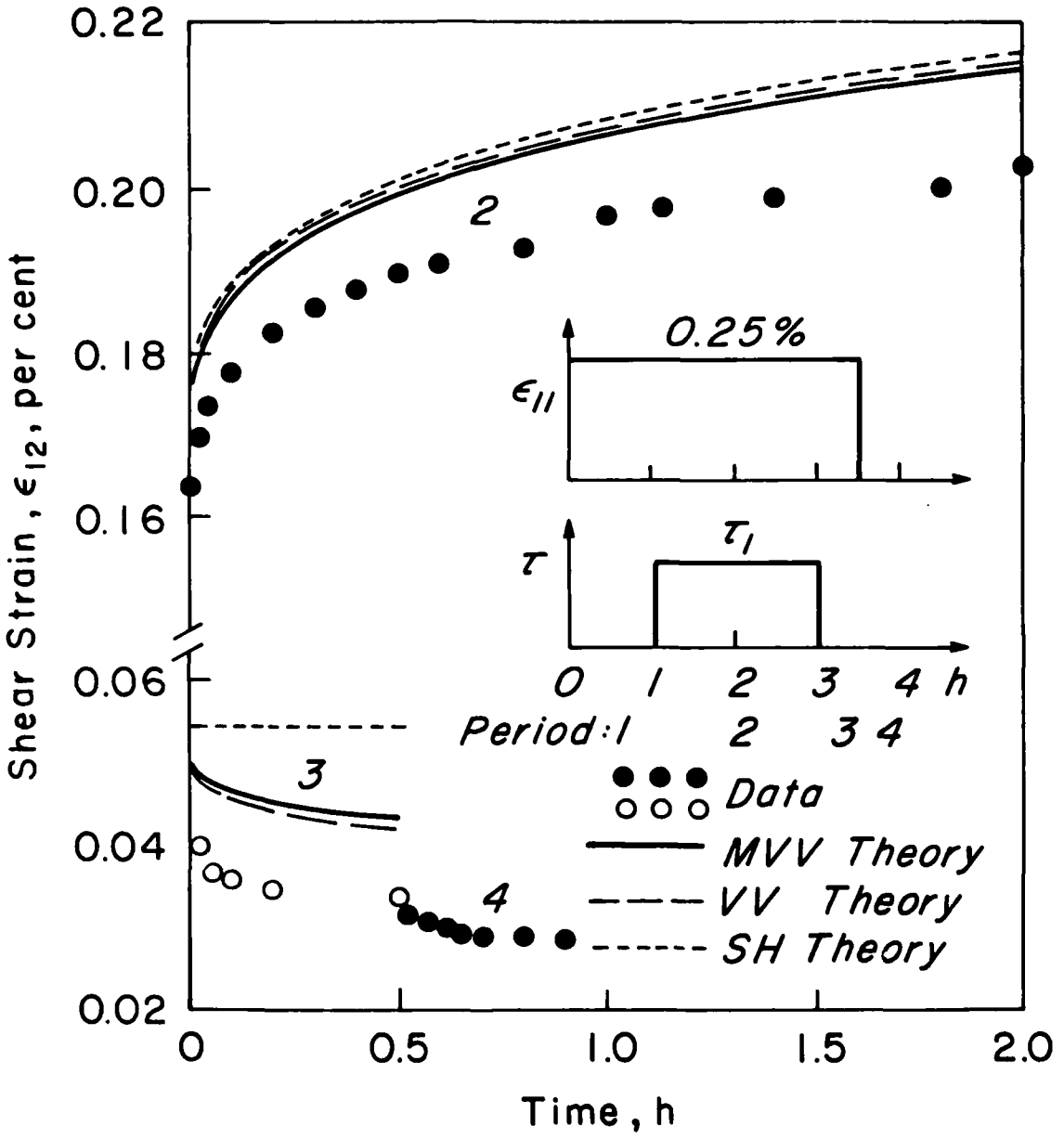
0.22
0.20
0.18
0.16
0.06
0.04
0.02
0
0.5
1.0
1.5
2.0
Time, h
Shear Strain, ϵ_{12}, per cent
2
3
4
0.25%
ϵ_{11}
τ
τ_1
0 1 2 3 4 h
Period: 1 2 3 4
Data
MVV Theory
VV Theory
SH Theory

FIGURE 2B

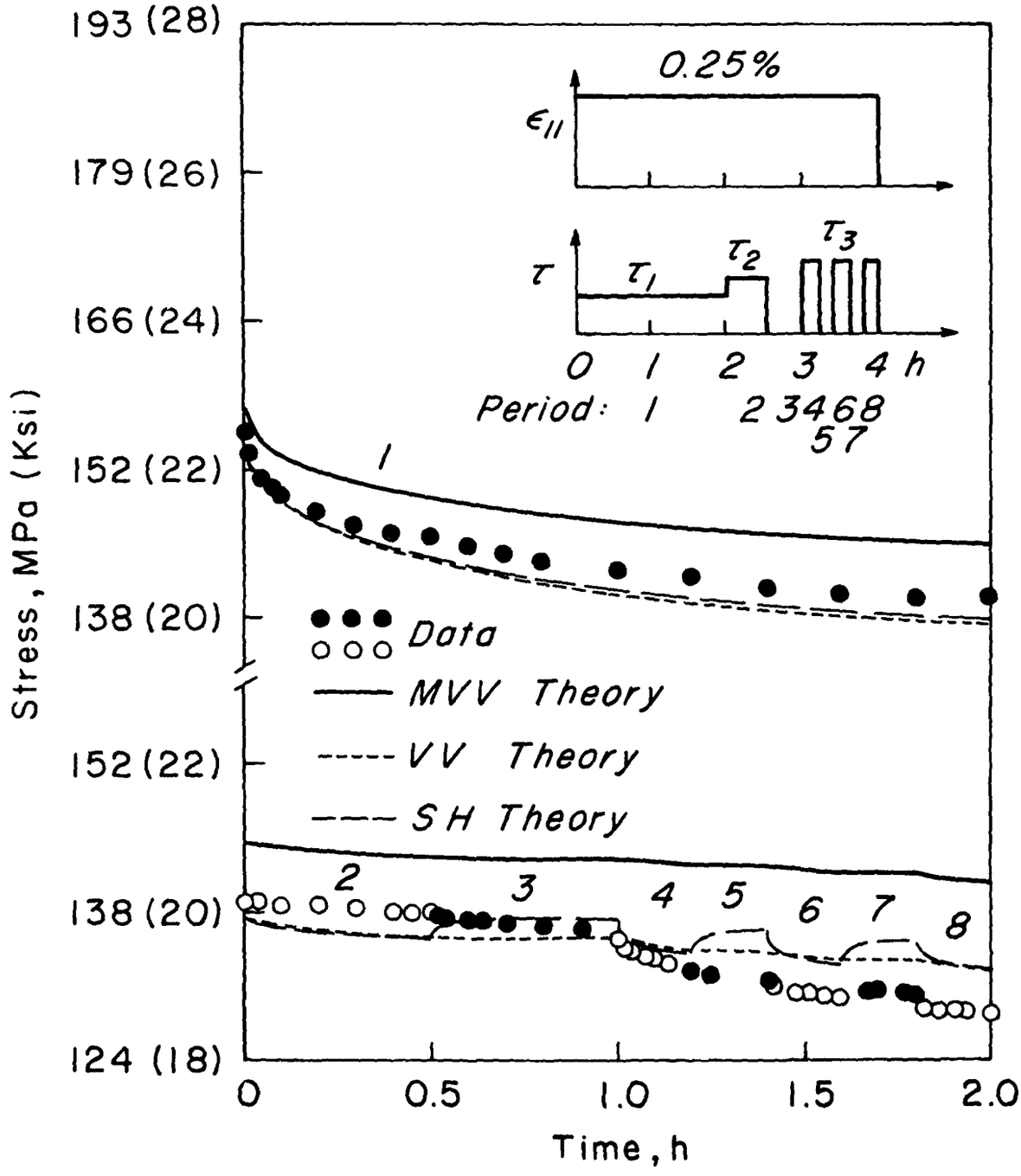
193 (28)
179 (26)
166 (24)
152 (22)
138 (20)
152 (22)
138 (20)
124 (18)
Stress, MPa (Ksi)
0.25%
ϵ_{11}
τ
τ_1
τ_2
τ_3
0 1 2 3 4 h
Period: 1 2 3 4 6 8 5 7
1
Data
MVV Theory
VV Theory
SH Theory
2
3
4
5
6
7
8
0
0.5
1.0
1.5
2.0
Time, h

FIGURE 3A

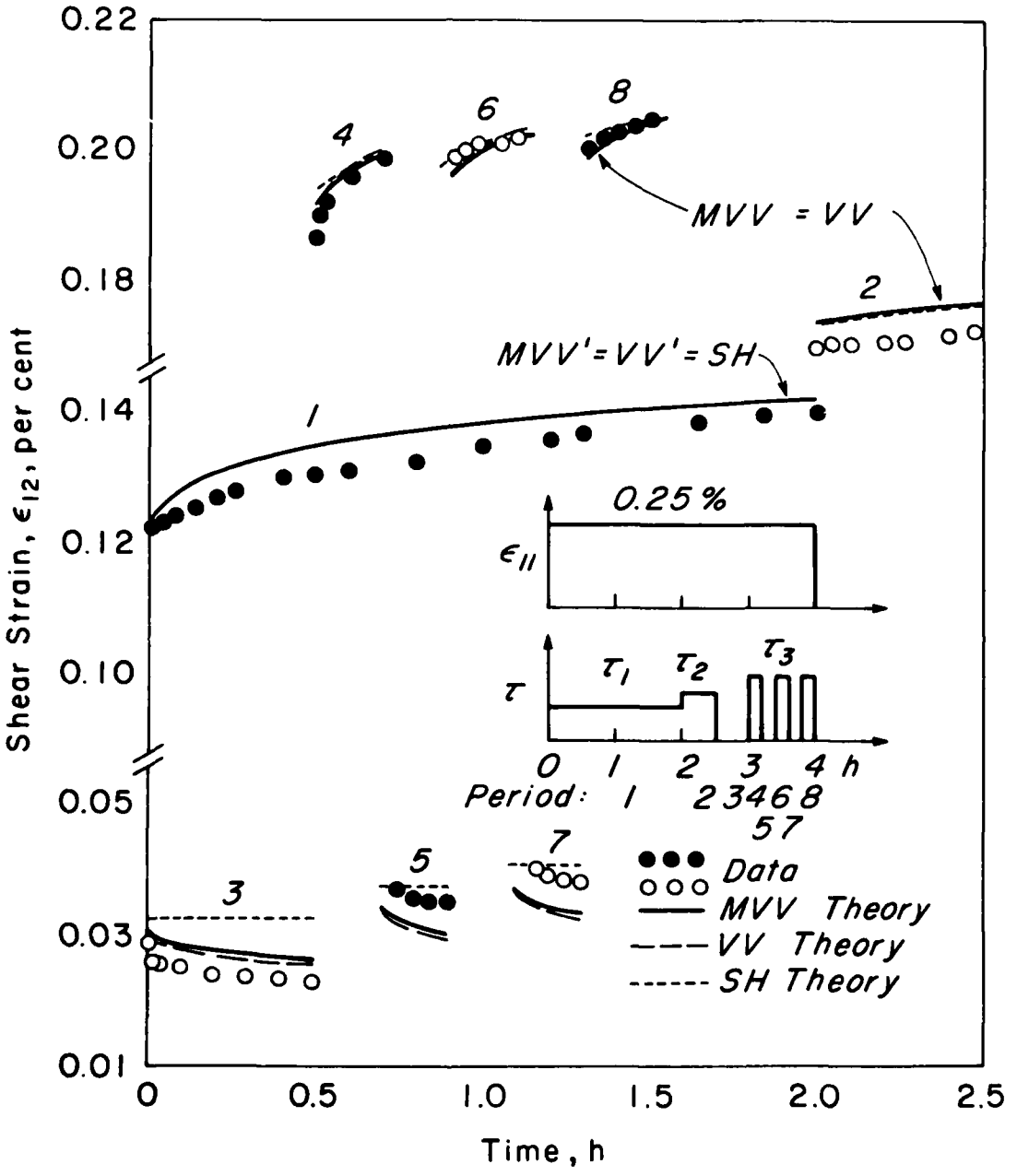
0.22
0.20
0.18
0.14
0.12
0.10
0.05
0.03
0.01
Shear Strain, ϵ_{12}, per cent
0
0.5
1.0
1.5
2.0
2.5
Time, h
4
6
8
MVV = VV
2
MVV'=VV'=SH
1
0.25 %
ϵ_{11}
τ
τ_1
τ_2
τ_3
0 1 2 3 4 h
Period: 1 2 3 4 6 8 5 7
3
5
7
Data
MVV Theory
VV Theory
SH Theory

FIGURE 3B

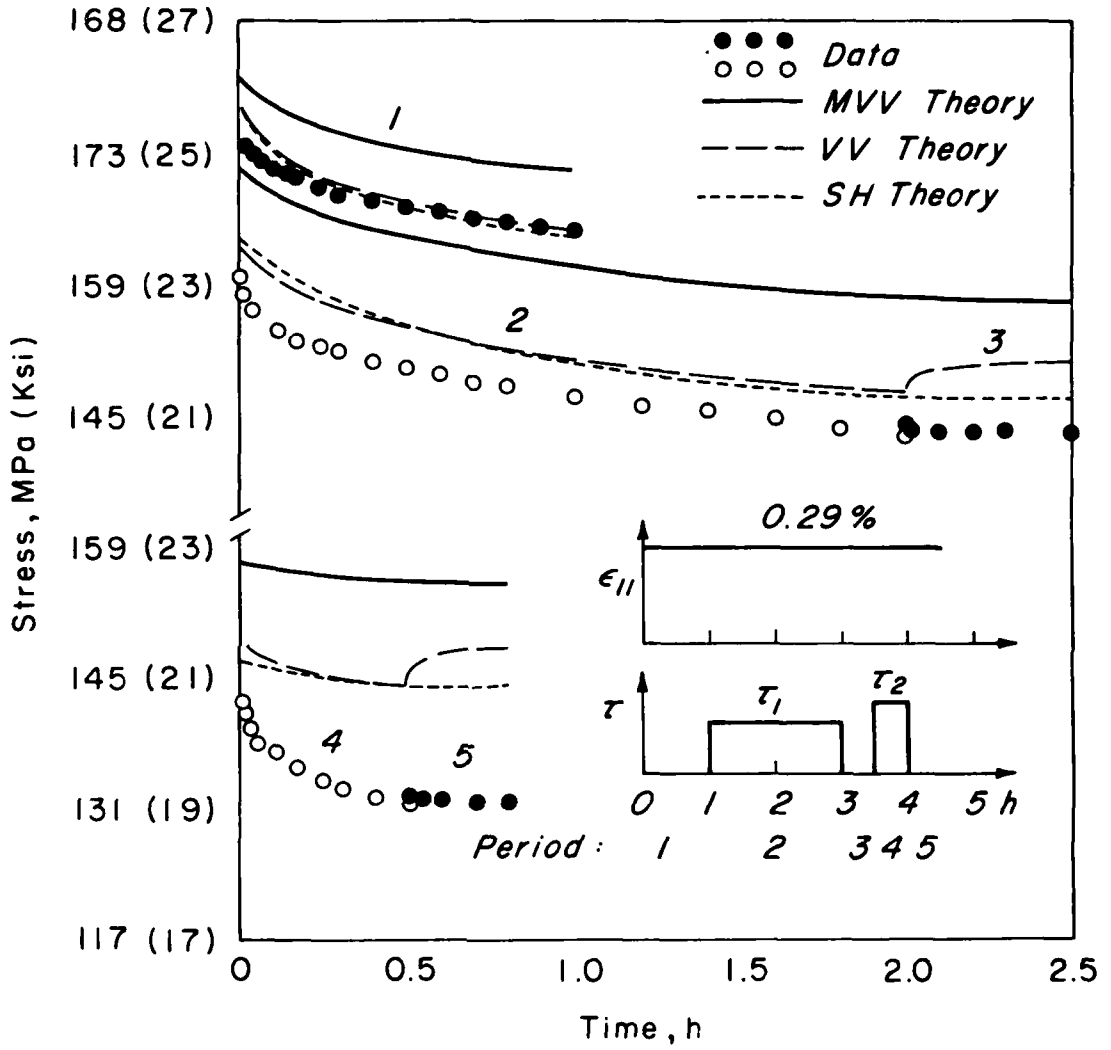
168 (27)
173 (25)
159 (23)
145 (21)
159 (23)
145 (21)
131 (19)
117 (17)
Stress, MPa (Ksi)
0
0.5
1.0
1.5
2.0
2.5
Time, h
Data
MVV Theory
VV Theory
SH Theory
1
2
3
4
5
0.29 %
ϵ_{11}
τ
τ_1
τ_2
0 1 2 3 4 5 h
Period : 1 2 3 4 5

FIGURE 4A

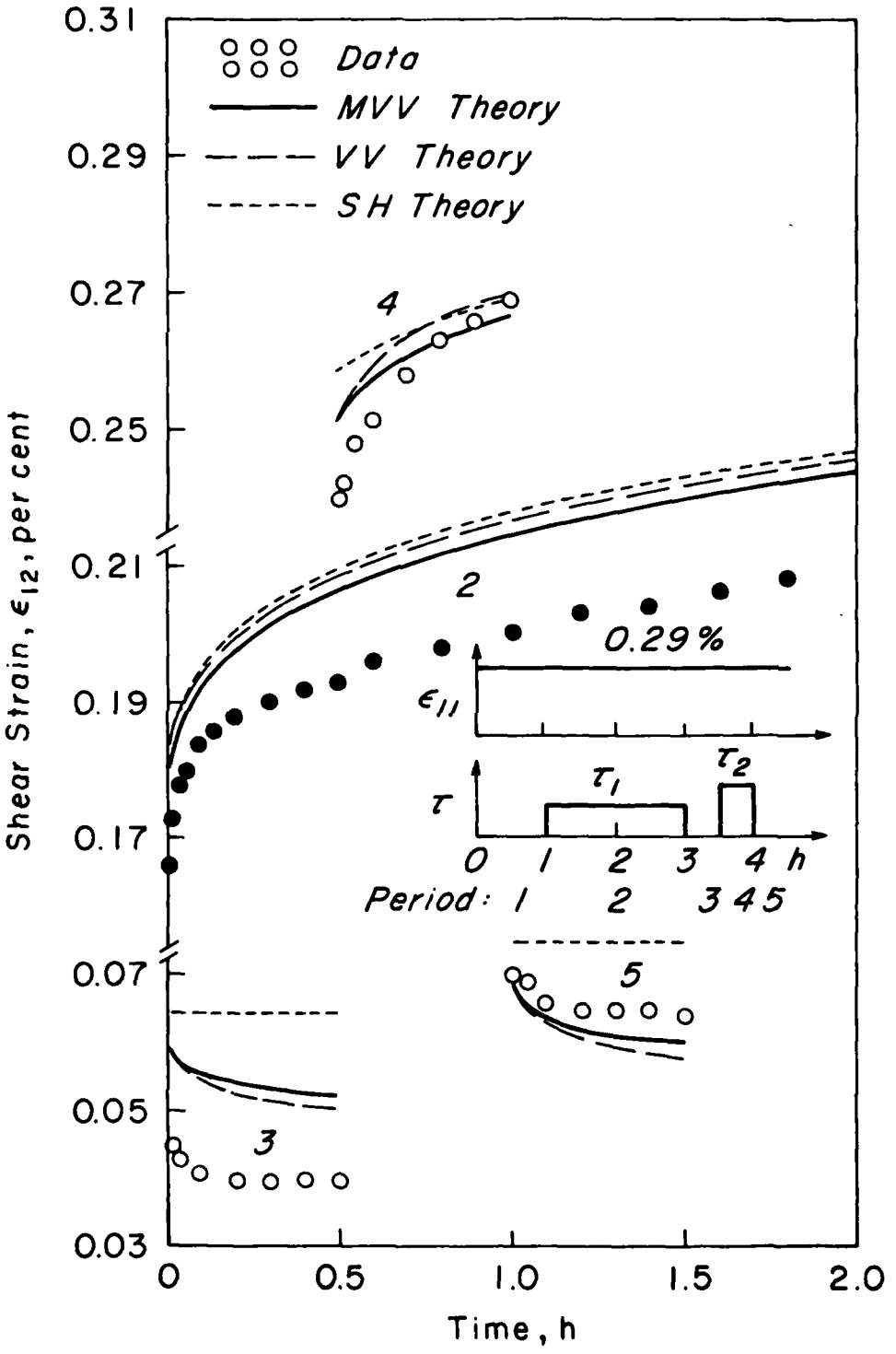
0.31
0.29
0.27
0.25
0.21
0.19
0.17
0.07
0.05
0.03
Data
MVV Theory
VV Theory
SH Theory
4
2
0.29%
ϵ_{11}
τ
τ_1
τ_2
0 1 2 3 4 h
Period: 1 2 345
5
3
Shear Strain, ϵ_{12}, per cent
0
0.5
1.0
1.5
2.0
Time, h

FIGURE 4B

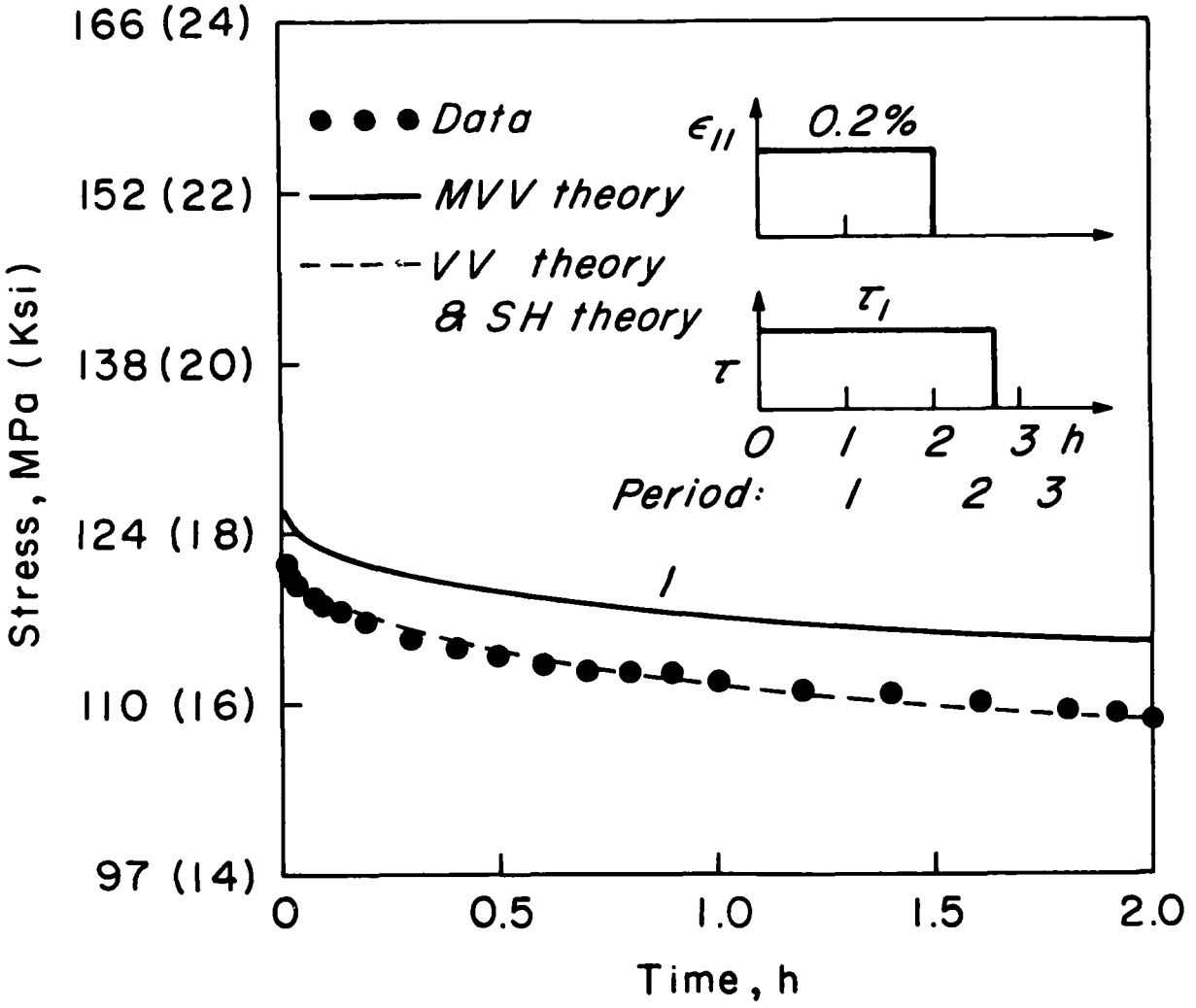
166 (24)
152 (22)
138 (20)
124 (18)
110 (16)
97 (14)
Stress, MPa (Ksi)
0
0.5
1.0
1.5
2.0
Time, h
Data
MVV theory
VV theory
& SH theory
ϵ_{11}
0.2%
τ_1
τ
0 1 2 3 h
Period: 1 2 3
1

FIGURE 5A

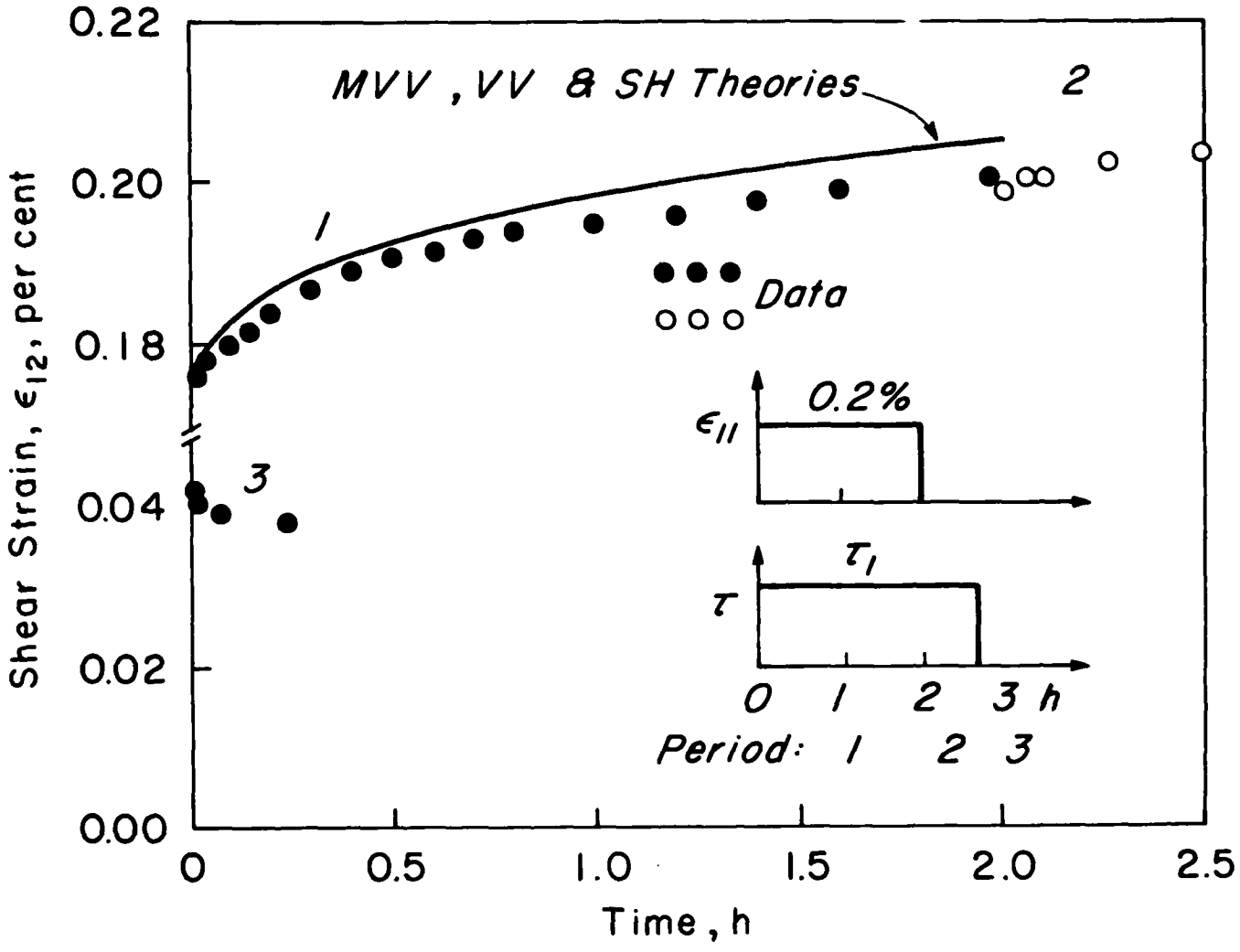
0.22
0.20
0.18
0.04
0.02
0.00
Shear Strain, ϵ_{12}, per cent
MVV , VV & SH Theories
2
1
Data
3
ϵ_{11}
0.2%
τ_1
τ
0 1 2 3 h
Period: 1 2 3
0
0.5
1.0
1.5
2.0
2.5
Time , h

FIGURE 5B

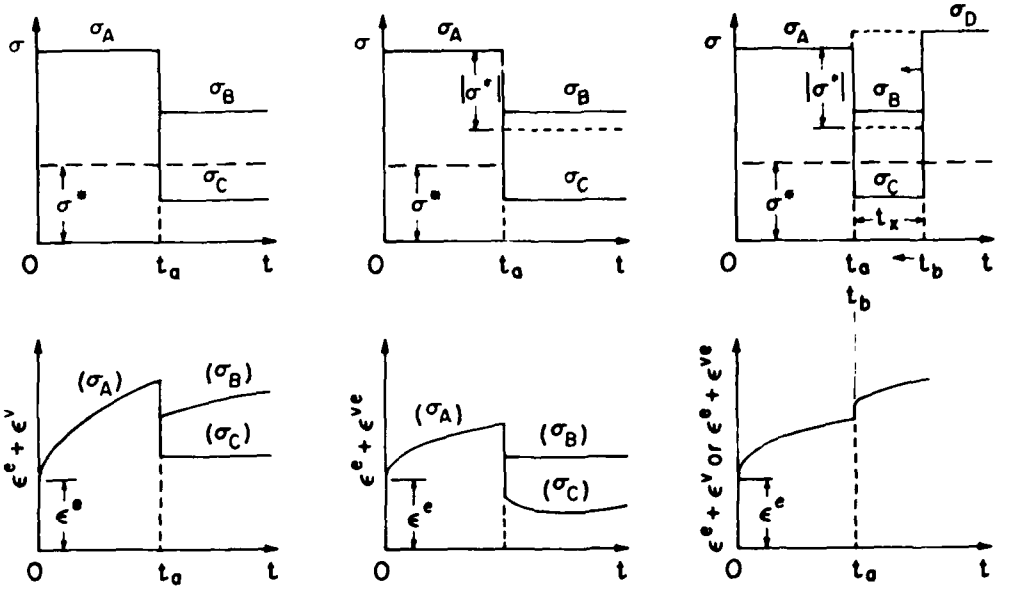

(a) Nonrecoverable Strain, Partial Unloading at t_a:

$\sigma_B < \sigma^*, \dot{\epsilon}^v > 0,$

$\sigma_C \le \sigma^*, \dot{\epsilon}^v = 0,$

(b) Recoverable Strain, ϵ^{ve}; Partial Unloading at t_a:

$\sigma_A - \sigma_B \le |\sigma^*|, \dot{\epsilon}^{ve} = 0,$

$\sigma_A - \sigma_C > |\sigma^*|, \dot{\epsilon}^{ve} \neq 0.$

(c) Reloading, at t_b; Nonrecoverable Strain, ϵ^v;

$\sigma_C \le \sigma^* < \sigma_D.$

Time t_b Shifted.

Recoverable Strain, ϵ^{ve};

$\sigma_D > \sigma_A > \sigma_B,$

$\sigma_A - \sigma_B \le |\sigma^*|,$

Time t_b Shifted.

FIGURE 6

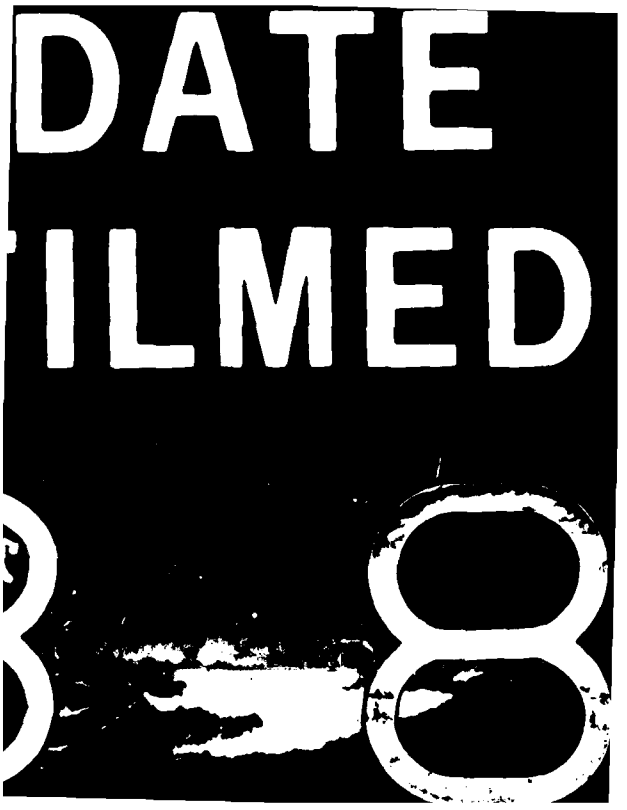
DATE
ILMED